Title

Image-guided high-dose-rate brachytherapy: preliminary outcomes and toxicity of a joint interventional radiology and radiation oncology technique for achieving local control in challenging cases.

Journal

Journal of contemporary brachytherapy, 7(5)

ISSN

1689-832X

Authors

Kishan, Amar U
Lee, Edward W
McWilliams, Justin
et al.

Publication Date

2015-10-01

DOI

10.5114/jcb.2015.54947

Peer reviewed

Original paper

Image-guided high-dose-rate brachytherapy: preliminary outcomes and toxicity of a joint interventional radiology and radiation oncology technique for achieving local control in challenging cases

Amar U. Kishan, MD[1], Edward W. Lee, MD, PhD[2], Justin McWilliams, MD[2], David Lu, MD[2], Scott Genshaft, MD[2], Kambiz Motamedi, MD[2], D. Jeffrey Demanes, MD[1], Sang June Park, PhD[1], Mary Ann Hagio, CMD[1], Pin-Chieh Wang, PhD[1], Mitchell Kamrava, MD[1]

[1]Department of Radiation Oncology, [2]Department of Interventional Radiology, David Geffen School of Medicine, University of California, Los Angeles, California, USA

Abstract

Purpose: To determine the ability of image-guided high-dose-rate brachytherapy (IG-HDR) to provide local control (LC) of lesions in non-traditional locations for patients with heavily pre-treated malignancies.

Material and methods: This retrospective series included 18 patients treated between 2012 and 2014 with IG-HDR, either in combination with external beam radiotherapy (EBRT; n = 9) or as monotherapy (n = 9). Lesions were located in the pelvis (n = 5), extremity (n = 2), abdomen/retroperitoneum (n = 9), and head/neck (n = 2). All cases were performed in conjunction between interventional radiology and radiation oncology. Toxicity was graded based on CTCAE v4.0 and local failure was determined by RECIST criteria. Kaplan-Meier analysis was performed for LC and overall survival.

Results: The median follow-up was 11.9 months. Two patients had localized disease at presentation; the remainder had recurrent and/or metastatic disease. Seven patients had prior EBRT, with a median equivalent dose in 2 Gy fractions (EQD_2) of 47.0 Gy. The median total EQD_2s were 34 Gy and 60.9 Gy for patients treated with monotherapy or combination therapy, respectively. Image-guided high-dose rate brachytherapy was delivered in one to six fractions. Six patients had local failures at a median interval of 5.27 months with a one-year LC rate of 59.3% and a one-year overall survival of 40.7%. Six patients died from their disease at a median interval of 6.85 months from the end of treatment. There were no grade ≥ 3 acute toxicities but two patients had serious long term toxicities.

Conclusions: We demonstrate a good one year LC rate of nearly 60%, and a favorable toxicity profile when utilizing IG-HDR to deliver high doses of radiation with high precision into targets not readily accessible by other forms of local therapy. These preliminary results suggest that further studies utilizing this approach may be considered for patients with difficult to access lesions that require LC.

J Contemp Brachytherapy 2015; 7, 5: 327-335
DOI: 10.5114/jcb.2015.54947

Key words: image-guided brachytherapy, local control, palliation.

Purpose

The multidisciplinary oncology team possesses a wide armamentarium of tools for achieving local tumor control, including thermal and other direct ablation techniques performed by interventional radiologists and external beam radiation therapy (EBRT) – based techniques delivered by the radiation oncologist [1, 2]. While these both offer excellent local control (LC) with acceptable toxicity for appropriately selected patients, there remain scenarios in which achieving LC is challenging. For IR-based ablative techniques these include lesions in close proximity to the vasculature and/or organs-at-risk (OARs) [3] and larger lesions [4, 5]. For EBRT-based ablative techniques, the main limitations are lesion size and proximity to critical OARs [6, 7, 8].

Address for correspondence: Mitchell Kamrava, MD, Asst. Prof., Department of Radiation Oncology, David Geffen School of Medicine, University of California, Los Angeles, 200 UCLA Medical Plaza, B265, Los Angeles, CA 90095, USA, phone: +1 310 825 9771, fax: +1 310 794 9795, e-mail: mkamrava@mednet.ucla.edu

Received: 10.08.2015
Accepted: 03.10.2015
Published: 31.10.2015

Image-guided interstitial high-dose-rate (IG-HDR) brachytherapy can overcome some of the limitations of both IR-based and EBRT-based ablative techniques [9]. With IG-HDR, a collaborative effort between interventional radiologists and radiation oncologists allows delivery of high doses of radiation via catheters placed directly into the target lesion. The sharp dose gradients and intra-tumoral heterogeneity provided by HDR allows for simultaneous dose-escalation and OAR sparing. There are multiple clinical reports using IG-HDR to treat hepatic lesions [10, 11, 12, 13, 14, 15, 16, 17, 18, 19, 20], recurrent anorectal cancer [21, 22, 23, 24], lung [25], head/neck cancer [26, 27, 28, 29], and metastatic melanoma deposits in various locations [30]. Aside from the latter report, however, other reports on the use of IG-HDR to target a variety of locations in order to provide local control in patients with locally advanced or incurable disease are sparse. We describe the clinical outcomes of a series of 18 patients treated with IG-HDR in a wide variety of disease sites, either in combination with a course of EBRT or as monotherapy.

Material and methods

Brachytherapy planning and delivery

An institutional review board waiver was approved prior to conducting the present retrospective study. Eighteen patients treated at the Department of Radiation Oncology at the University of California Los Angeles between 2012 and 2014 were identified. All patients were deemed to be inappropriate candidates for a purely interventional radiology-based ablative approach or EBRT approach for the lesion in question. These other approaches were generally deemed inappropriate due to large size of disease and/or proximity to normal organs at risk with the small bowel being the most common limiting organ at risk. Briefly, a team of radiation oncologists and interventional radiologists performed the IG-HDR procedures. Patients were placed under sedation, and both physicians selected the number and trajectory of 15G flexi-guide catheters to be placed into the target under image-guidance (ultrasound, CT, or both). A pre-implantation plan was used for non-abdominal lesions; due to small bowel variation, pre-implantation plans were not used for abdominal lesions. Planning target volumes and OARs were contoured by the radiation oncologist using images obtained from a post-implantation CT simulation scan. Treatment planning was performed using the inverse planning simulation annealing algorithm from Oncentra Brachy Treatment Planning System Version 4.3 (Nucletron, an Elekta company, Elekta AB, Stockholm, Sweden). Manual graphical optimization was performed prior to final plan approval. Prescription doses were chosen conservatively on the basis of clinical judgment. Planning was performed with the goal of delivering a dose covering the target being greater than 90% of the prescription dose. Depending on the number of fractions prescribed, the patient either completed treatment later that day or was admitted to the hospital overnight for further fractions the following day. Patients receiving more than one fraction had at least six hours in between treatments. A repeat CT simulation scan was performed prior to each fraction and appropriate catheter adjustments were made as necessary. For the purposes of comparison, an equivalent dose in 2 Gy fractions (EQD_2) was calculated for each patient, utilizing the formula EQD_2 = (dose/fraction*number of fractions)*((dose/fraction + α/β)/(2 + α/β)), where α/β refers to tumor radiosensitivity and is set to 10 [31].

Table 1. Baseline patient characteristics

Age (median, range)	62 (17-87)
Gender	
Male (*n*)	9
Female (*n*)	10
Lesion size (mean, range) (cm)	
Pelvis (*n* = 5)	5.4 (1.5-13.3)
Extremity (*n* = 2)	6.5 (2.5-10.5)
Abdomen/Retroperitoneum (*n* = 9)	6.1 (1.5-12)
Head/Neck (*n* = 2)	4.8 (3.4-6.2)
Prior EBRT (*n*)	7
Time from prior EBRT (months)	17.2 (7.7-82.7)
Prior EBRT EQD_2 (Gy)	47.0 (44.3-56)
Combination EBRT course* (*n*)	8
Combination EBRT EQD_2 (Gy) (median, range)	44.3 (44.3-44.3)
Combination EBRT with chemotherapy (*n*)	3
Prior receipt of chemotherapy (*n*)	14
Adjuvant chemotherapy (*n*)	12

**Patients who received combination external beam radiotherapy (EBRT) courses are those for whom image-guided brachytherapy was performed as a boost following EBRT.*
EBRT – external beam radiation therapy; EQD_2 – equivalent dose in 2 Gy; n – number

Toxicity and follow-up analysis

All patients had follow-up imaging with CT or MRI at least three months after treatment, were assessed by a clinician within 12-16 weeks and generally at three month intervals thereafter. Acute toxicity was graded utilizing the Common Terminology Criteria for Adverse Events (CTCAE) version 4 [32], and was derived from a retrospective review of follow-up notes. Chronic toxicities (defined as occurring > 90 days after IG-HDR) were also graded in this fashion. All follow-up dates were measured from the date of IG-HDR. Local control was determined on the basis of RECIST criteria [33] with progressive disease categorized as local failure and all other responses (stable disease and either partial or complete response) treated as LC. A Kaplan-Meier analysis was conducted to model LC and overall survival probability.

Results

Patient and treatment characteristics

The median clinical follow-up was 11.9 months (range: 4.0-28.5); the median imaging follow-up was 9.15 months (range: 3.5-28.5). Patient baseline characteristics

are shown in Table 1. Detailed information on the dose/fractionation regimens for each patient are shown in Table 2 and clinical vignettes are provided in Table 3. Two patients presented for IG-HDR with primary locally advanced disease; the remaining 16 patients had locally recurrent and/or metastatic disease at presentation. Seven patients had prior EBRT that included the target lesion with a median EQD_2 of 47.0 Gy and a median treatment interval of 17.2 months. Nine patients received IG-HDR in combination with a course of EBRT (median EQD_2 of 49.6 Gy for concurrent EBRT doses).

Sample plans are shown in Figure 1, and average target dosimetry is shown in Table 4. The average number of catheters used per case ranged from 7 to 15, depending on site (averages of 15 for pelvis, 13 for extremity, 7 for abdomen/retroperitoneum, and 12 for head/neck). In general, the number of catheters used per case decreased over time as experience was accumulated. Dose fractionation schema varied but the overall average EQD_2 delivered by IG-HDR was 34 Gy for patients treated with IG-HDR alone, and 16.7 Gy for patients who also received EBRT. The median total EQD_2 for patients treated with combination IG-HDR and EBRT was 60.9 Gy. For the overall population, median EQD_2 was 54.2 Gy.

Clinical outcomes

Six patients had local failures. The median time to local failure was 4.07 months (range: 1.0-23.2); among patients without local failure, the median imaging follow-up was 6.92 months (range: 3.47-28.47). Five patients had distant progression or developed new metastases after IG-HDR, at a median interval of 2.17 months (range: 1.03-11.67). Six patients died from their disease, with a median interval of 6.85 months (range: 4.50-23.17). Two of these patients had no metastases at the time of death, while three had metastatic disease at presentation and one developed metastatic disease after IG-HDR, Kaplan-Meier curves of LC and overall survival are shown in Figure 2, demonstrating a one-year LC rate of 59.3% and a one-year overall survival of 40.7%.

Two of the nine patients with abdominal/retroperitoneal lesions had local failures (22.2%), compared with neither of the two patients with extremity lesions (0%), one of two patients with head/neck lesions (50%), and three of five patients with pelvic lesions (60%). Four of seven patients who received a total $EDQ_2 < 45$ Gy had local failures (57.1%), compared with two out of eleven treated with an $EQD_2 > 45$ Gy (18.1%). Five out of nine patients treated with IG-HDR alone had local failures

Table 2. Dose/fractionation data

Patient	Lesion location	IG-HDR dose/fractionation	Combination EBRT dose/fractionation	IG-HDR + combination EQD_2 (Gy)*	Total cumulative EQD_2 (Gy)**
1	Pelvis	7 Gy × 3		29.8	82.9
2	Pelvis	5 Gy × 2	1.8 Gy × 25	56.8	56.8
3	Pelvis	3 Gy × 3	1.8 Gy × 25	54	54
4	Pelvis	8.5 Gy × 1, 12.5 Gy × 1		59.3	86.1
5	Pelvis	5.5 Gy × 5		35.5	79.8
6	Extremity	3.75 Gy × 4	1.8 Gy × 25	84.3	140.4
7	Extremity	6 Gy × 5		17.2	17.2
8	Abdomen/Retroperitoneum	10 Gy × 1	1.8 Gy × 25	60.9	60.9
9	Abdomen/Retroperitoneum	10 Gy × 1	1.8 Gy × 25	60.9	60.9
10	Abdomen/Retroperitoneum	6 Gy × 1		8	8
11	Abdomen/Retroperitoneum	5.5 Gy × 2	1.8 Gy × 25	58.5	58.5
12	Abdomen/Retroperitoneum	18 Gy × 1	1.8 Gy × 25	86.3	86.3
13	Abdomen/Retroperitoneum	13 Gy × 2		49.8	49.8
14	Abdomen/Retroperitoneum	16 Gy × 1		34.7	34.7
15	Abdomen/Retroperitoneum	10 Gy × 2		33.3	77.6
16	Abdomen/Retroperitoneum	7 Gy × 1	1.8 Gy × 25	54.2	54.2
17	Head/Neck	6 Gy × 6		48	118.8
18	Head/Neck	10 Gy ×1	6 Gy × 5	56.7	56.7

IG-HDR – image-guided high-dose-rate brachytherapy, EBRT – external beam radiotherapy
**EQD_2 – equivalent dose in 2 Gy fractions; this was calculated for each patient, utilizing the formula EQD_2 = (dose/fraction*number of fractions)*((dose/fraction + α/β)/(2 + α/β)), where α/β refers to tumor radiosensitivity and is set to 10.*
***Total cumulative EQD_2 incorporates dose from prior treatment.*

Table 3. Case vignettes

Patient	Clinical summary
1	61M who presented with recurrent rectal adenocarcinoma, manifesting as an unresectable 6.5 × 7.1 × 13.3 cm pelvic lesion eroding through skin. He initially presented with T4bN1M0 rectal adenocarcinoma s/p neoadjuvant chemoradiation, an abdominoperineal resection, and adjuvant capecitabine for six cycles. Brachyablation was performed 11.4 months after prior EBRT.
2	61F who presented with newly diagnosed T4aN1M1 squamous cell carcinoma of the vagina. She had a 3.59 cm right pelvic sidewall soft tissue implant at presentation. She underwent concurrent chemoradiation followed by an interstitial HDR brachytherapy boost to residual vaginal disease and a left inguinal node prior to brachyablation of the right sidewall implant.
3	82F who presented with newly diagnosed T4N1M0 squamous cell carcinoma of the vagina with a left pelvic node measuring 1.5 cm. She underwent EBRT to the pelvis alone, followed by an interstitial HDR boost to the vagina concurrent with brachyablation to the left pelvic node.
4	60F who presented with recurrent endometrial adenocarcinoma, manifesting as an unresectable 5.1 × 4.4 cm left pelvic sidewall mass. She had originally presented with FIGO Stage II grade 1 disease, and was treated with surgical resection followed by adjuvant chemotherapy and whole pelvis EBRT with a vaginal cuff brachytherapy boost. She developed left pelvic lymphadenopathy two years later, which ultimately became refractory to systemic therapy after an initial period of response. She underwent brachyablation of the pelvic sidewall lesion nearly 61 months after her prior EBRT because of local progression, she underwent a second brachyablation procedure 2.93 months later.
5	66M who presented with recurrent rectal adenocarcinoma, manifesting as an unresectable 2.4 × 3.3 cm lesion within the rectal lumen of his Hartmann pouch with partial involvement of the sphincter. He initially presented with T3N0M1 rectal adenocarcinoma (with two liver metastases), for which he underwent preoperative chemoradiotherapy followed by simultaneous wedge resection and abdominoperineal resection, and six cycles of adjuvant chemotherapy. Seventeen months later, he developed the local recurrence in question. He received brachyablation 22.9 months after the prior EBRT.
6	17M who presented with an unresected 10.5 cm synovial sarcoma of the left medial plantar surface of the foot. He had initially presented several months prior with pulmonary metastases; he underwent six cycles of ifosfamide/doxorubicin chemotherapy with good response of his pulmonary lesions but not of the primary. He and his family refused surgery, and he was treated with EBRT followed by a brachyablation boost.
7	24M who presented with locally recurrent Ewing's sarcoma of the right proximal tibia. He initially presented eight years earlier, and refused surgery, opting for definitive radiotherapy sandwiched between multiple cycles of chemotherapy. He had first developed a local recurrence four years earlier and again refused surgery. He tried chemotherapy but developed pulmonary metastases and eventually underwent a palliative debulking procedure of the recurrent primary three years before presentation for brachyablation. Despite further chemotherapy, he continued to have progressive pulmonary disease and within 22 months, he had a local recurrence measuring 2.5 cm. He again refused surgery and brachyablation was performed, roughly 82.7 months after his initial course of radiation for his gross disease.
8	27F who presented with a 6.1 cm, unresectable ectopic renal clear cell carcinoma involving the head of the pancreas and distal duodenum. She received brachyablation prior to EBRT.
9	58F who presented with an 8 cm paraaortic recurrence of endometrial adenocarcinoma. She underwent surgical resection and vaginal cuff brachytherapy for FIGO stage IA grade 1 endometrial adenocarcinoma five years prior to consideration of brachyablation. Four years after the vaginal cuff brachytherapy, she developed a paraaortic recurrence. She underwent systemic treatment; though this initially stabilized the lesion, it began to progress, growing to 8 cm. She received chemoradiation, followed by brachyablation.
10	61M who presented with a 10.5 cm para-aortic/aortocaval metastatic pheochromocytoma lesion. He had been diagnosed with metastatic disease at initial presentation over 20 years prior and had undergone multiple radionuclide treatments. Upon first appearance of this lesion, he underwent several systemic therapies and multiple cryoablation treatments. Since these failed, he ultimately presented for brachyablation. He only tolerated one fraction due to anxiety.
11	80F who presented with a 5.2 × 4.9 cm aortocaval lesion secondary to recurrent uterine carcinosarcoma. She initially presented with FIGO stage II disease, for which she underwent surgical resection followed by one cycle of adjuvant chemotherapy, discontinued due to adverse effects. The recurrence developed shortly thereafter and she underwent EBRT alone, followed by brachyablation.
12	53F who presented with a 1.5 cm metastatic lesion in the right lobe of the liver, secondary to clear cell/endometrioid ovarian cancer. Her original disease had been treated with surgical resection and adjuvant chemotherapy eight years prior. She developed intra-abdominal metastases within one year of completing adjuvant chemotherapy, and had since undergone multiple cycles of chemotherapy and ablative procedures for a total of four intra-abdominal recurrences. She presented for brachyablation with the aforementioned hepatic lesion as well as synchronous para-aortic lymphadenopathy once these lesions were determined to be refractory to chemotherapy. She underwent EBRT to the para-aortic region, followed by brachyablation to the right hepatic lobe lesion.

Table 3. Cont.

Patient	Clinical summary
13	87F who presented with a 5.5 cm right flank mass secondary to metastatic clear cell renal carcinoma, She was initially treated with a right nephrectomy nearly a decade earlier; At the time of recurrence, she was considered to not be a surgical candidate and thus presented for brachyablation.
14	62F who presented with a 2.8 cm left peri-renal lesion secondary to metastatic small bowel leiomyosarcoma. She presented with metastatic disease six months earlier and had completed chemotherapy one month prior to consideration of brachyablation. The peri-renal lesion in question showed no response to chemotherapy, though her other intra-abdominal lesions had responded.
15	66F who presented with a 2.9 cm para-aortic nodal recurrence from endometrial papillary serous carcinoma. She had initially presented with FIGO stage IIIB disease, which was treated with neoadjuvant chemoradiation, followed by surgical resection, a vaginal brachytherapy boost, and adjuvant chemotherapy. She developed a left paraspinous recurrence 21 months later and was treated with palliative radiotherapy followed by chemotherapy. Upon completing, she developed ureteral stenosis secondary to the aforementioned para-aortic node. She underwent brachyablation 7.7 months after completing her second course of radiotherapy.
16	20M who presented with an 11.7 cm unresectable recurrent desmoid tumor. The patient initially presented 10 years earlier, shortly after diagnosis of Gardner's syndrome. He was originally treated with surgical resection but ultimately had several local recurrences necessitating local ablative techniques and multiple chemotherapy trials. Two years prior to presentation for brachyablation, he experienced a recurrence that included the base of the small bowel mesentery and was thus unresectable; this lesion progressed on more aggressive systemic therapy, and he therefore underwent EBRT prior to a brachyablation boost.
17	77M who presented with an unresectable 3.4 cm nodal recurrence of head and neck squamous cell carcinoma, abutting the left internal carotid artery and with left sternocleidomastoid and paraspinous muscle involvement. He had presented ten months earlier with a poorly differentiated SCC of unknown primary origin involving a level II neck node. He underwent definitive chemoradiation and initially had a good response but by eight months was found to have the aforementioned recurrence. He underwent brachyablation 10.1 months after his initial course of chemoradiation. Due to local progression, he underwent a second brachyablation 4.23 months later.
18	76M with an unresectable 6.2 cm right supraclavicular mass secondary to a right upper chest melanoma. He initially presented with T1aN0 disease, which was treated with WLE alone 14 years prior to the recurrence in question. He eventually underwent axillary lymph node dissection, showing N3 disease; however, he refused adjuvant therapy of any kind. He was treated with EBRT followed by brachyablation.

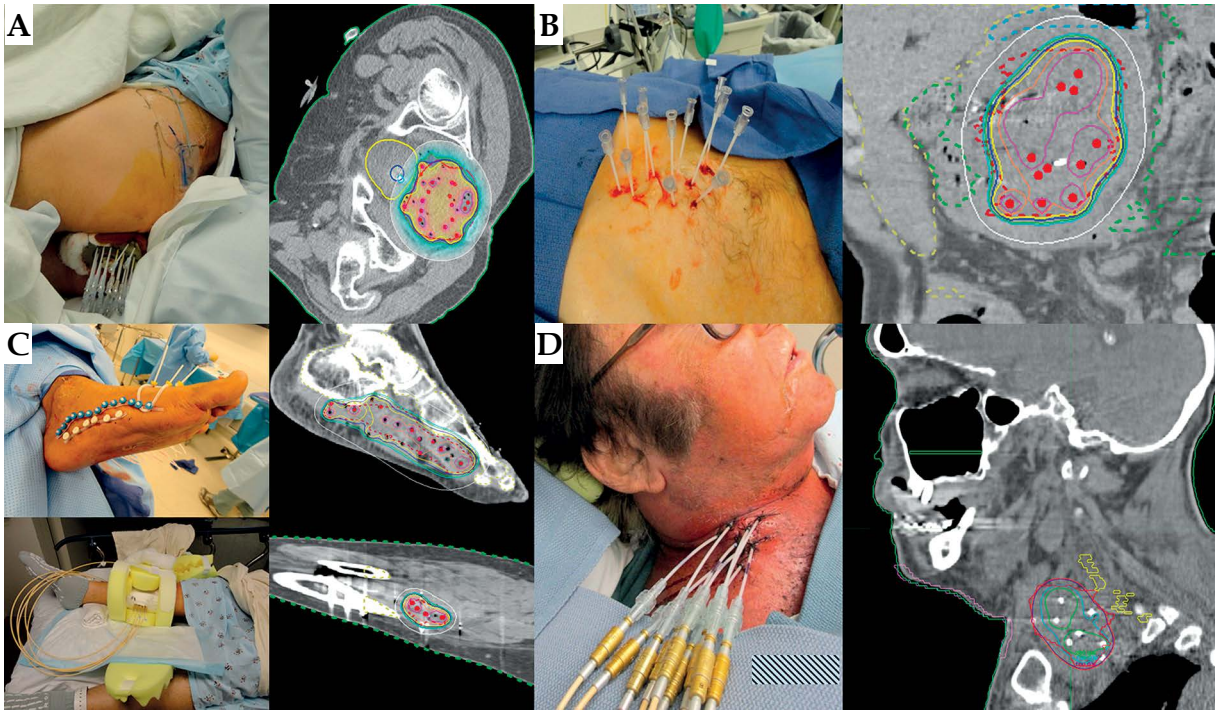

Fig. 1. Paired clinical photographs and image-guided high-dose-rate (IG-HDR) plans for five patients whose specific vignettes are found in the Supplementary Information section. (**A**) Patient 1, (**B**) patient 10, (**C**) top row, patient 6, bottom row, patient 7, (**D**) patient 19. The target volume is shown in red. The color code for the isodose colorwash is as follows: magenta, 200%; orange, 150%; yellow, 110%; dark blue, 100%; green, 90%, light blue, 85%

Table 4. Target coverage

Target parameter	Mean	Range
Planning target volume (ml)		
Pelvis (n = 5)	144.2	1.9-496
Extremity (n = 2)	56.5	14-99
Abdomen/Retroperitoneum (n = 9)	91.3	15-223
Head/Neck (n = 2)	46.1	42.9-48
$V_{100\%}$ (% of target volume receiving prescription dose)	88.7	69.6-100
$V_{150\%}$ (% of target volume receiving 150% of prescription dose)	52.9	29.7-90
$D_{90\%}$ (% of prescription dose covering 90% of target volume)	100.6	74.5-148

(55.6%), compared with one of nine patients (11.1%) treated with combination EBRT. Finally, four out of seven patients with prior EBRT had local failures (57.1%), compared with two out of eleven patients without prior EBRT (18.1%). Adjuvant chemotherapy did not appear to influence local control with local failures in one of six patients who did not receive adjuvant chemotherapy (16.7%) and five of 12 patients who did receive (41.7%).

Among patients who had LC, eight had stable disease and four had partial responses. Three of the patients who had local failures appear to have had "marginal misses", wherein disease progressed towards the edge of the 100% isodose line (an example is shown in Figure 3). Times to local failure were 1.03 and 2.87 months, respectively; two of these patients had repeat IG-HDR. One patient had a local failure (third recurrence overall) in 2.57 months and was treated with systemic therapy; she remains alive. The second had a local failure (third recurrence overall) in 8.37 months and passed away 2.47 months later.

Organ-at-risk dosimetry and toxicity

Organ-at-risk dosimetric parameters are shown in Table 5. Acute toxicities were minimal with five instances of grade 1 skin toxicity, three instances of grade 1 nausea, four instances of grade 1 diarrhea, four instances of grade 1 fatigue, and two instances of grade 1 pain. One patient had grade 2 diarrhea, another had grade 2 urinary frequency, one had grade 2 fatigue, and three had grade 2 pain. Another patient endorsed grade 2 anxiety after his first fraction, secondary to catheter placement. He discontinued treatment before his second and final fraction could be delivered. Otherwise, all patients who needed an overnight stay in the hospital tolerated having the brachytherapy catheters left in place overnight. No acute grade 3 or higher toxicities were seen.

With regards to chronic toxicity, one patient developed pelvic-cutaneous and vesico-perineal fistulas. Before IG-HDR was performed, the patient had prior chemoradiation and an abdominoperineal resection procedure, followed by adjuvant chemotherapy; at the time of IG-HDR, he had a bulky, painful local recurrence (Figure 4A). Subsequent to IG-HDR, he had a significant clinical response, with improvement in pain and significant reduction in tumor burden (Figure 4B). Unfortunately, he subsequently developed a bulky, painful local recurrence after his initial response, and it was at this point that the fistulization manifested (Figure 4C). The patient also began to receive bevacizumab infusions as a component of systemic therapy one month after IG-HDR, which may have also contributed to his fistula formation [34]. Another patient developed chronic grade 1 lower extremity weakness as well as bone necrosis. She had a history of EBRT to the pelvis and due to progressive disease after IG-HDR, she underwent a second course 2.93 months later. Both patients had bulky local recurrences that likely contributed to these sequelae.

Discussion

Despite significant technological improvements in both interventional radiology and radiation oncology, achieving LC remains challenging in certain scenarios, whether due to lesion size, proximity to critical structures, prior treatments, or a combination of the above.

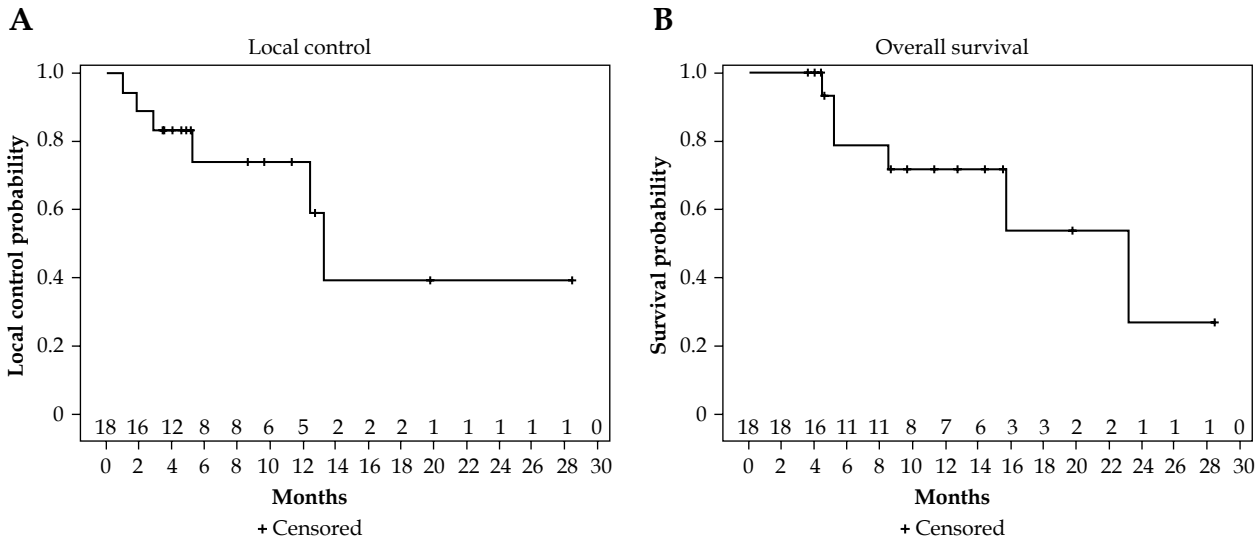

Fig. 2. Kaplan-Meier curves for local control and overall survival. The numbers at risk are shown at the bottom of the plot

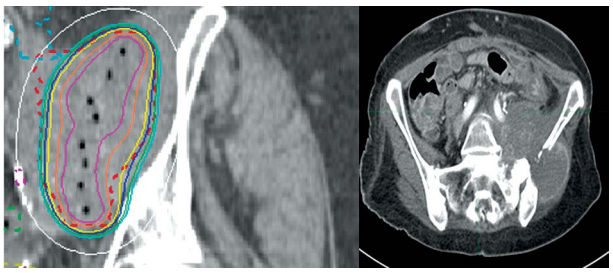

Fig. 3. The image-guided high-dose-rate (IG-HDR) plan for patient 4 (shown on the left) is compared to a two-month follow-up scan on the right, demonstrating growth of a lesion on the lateral surface of the ischium and eroding through the bone into the pelvic sidewall. At the time of presentation for IG-HDR, disease was only visible medial to the ischium, and hence the bone itself was not targeted. The color code for the isodose colorwash is as follows: magenta, 200%; orange, 150%; yellow, 110%; dark blue, 100%; green, 90%, light blue, 85%

Table 5. Organ-at-risk dosimetric parameters from image-guided high-dose-rate brachytherapy (IG-HDR) plan

Organ-at-risk	Dosimetric parameter (Gy)		
	$D_{0.1cc}$*	D_{1cc}	D_{2cc}
Pelvis (*n* = 5)			
Small bowel	4.66	3.79	3.46
Sigmoid	0.355	0.255	0.215
Rectum	1.64	1.34	1.20
Bladder	3.02	2.72	2.49
Urethra	3.02	2.46	1.68
Extremity (*n* = 2)			
Skin	2.63	2.28	2.18
Bone	5.73	4.72	4.14
Abdomen/Retroperitoneum (*n* = 9)			
Small bowel	5.97	4.99	4.60
Ipsilateral kidney	5.43	4.53	4.11
Liver	2.11	1.72	1.56
Spinal cord	3.86	3.33	3.08
Head and neck (*n* = 2)			
Skin	5.035	4.27	3.835
Mandible	1.65	1.32	1.21
Spinal cord	3.14	1.96	1.55

$D_{x\,cc}$ – maximum dose in Gy to "x" cc of the structure in question (where x = 0.1, 1, or 2 cc)

While essential in the upfront treatment of localized disease, achieving LC is also important in the recurrent and/or metastatic settings for symptomatic improvement and, in the setting of oligometastatic disease, improved outcomes. Our data suggest that IG-HDR offers a nearly 60% chance of LC at one year in a heavily pre-treated population for whom neither a purely interventional radiology-based approach nor an EBRT approach were felt to be optimal. Of the eighteen patients treated, only two were treated for a localized primary, while the rest had recurrent lesions and/or systemic disease. Seven had prior EBRT and eight received EBRT in combination with IG-HDR. Acute toxicities were mild with no grade ≥ 3 toxicities noted, though one patient discontinued treatment halfway through due to anxiety. Two patients had grade 3 chronic toxicities; IG-HDR likely contributed but both patients also had bulky local recurrences contributing to their symptoms, and both had prior EBRT.

Several reports of outcomes following IG-HDR have been reported, primarily with regards to treating hepatic lesions [10, 11, 12, 13, 14, 15, 16, 17, 18, 19, 20], recurrent anorectal cancer [21, 22, 23, 24], lung lesions [25], and head/neck cancer [26, 27, 28, 29]. Series including more heterogeneous populations are limited. Bretschneider *et al*. recently reported the outcomes of 14 patients who received IG-HDR for metastatic melanoma lesions located in the liver, lung, adrenals, lymph nodes, and kidneys [30]. The median lesion size was 1.5 cm, with a median dose of 19.9 Gy (EQD_2 of 45.9 Gy). They reported

Fig. 4. The clinical course for patient 1 is shown pictorially. On the left is the gross disease present at the time of IG-HDR treatment. Tumor burden 4.5 months after treatment is shown in the middle. Unfortunately, the patient had subsequent progression, resulting in bulky local recurrence, shown on the right at one year following IG-HDR

a median LC rate of 90% at five months. Image-guided interstitial high dose rate was well-tolerated, with two patients developing small pneumothoraces and one patient developing cholangitis. In general, the average diameter of the lesions treated in our cohort was larger at 5.8 cm (corresponding to an average planning target volume of 93.8 ml), and the average EQD_2 for lesions treated with IG-HDR monotherapy was 36 Gy. Despite these differences, our LC rate of 79% at five months is consistent with the results reported by Bretschneider *et al*. The generally large lesion size and high-risk composition of our cohort could also explain why our one-year LC rate of 59% is slightly lower than the reported results from the other aforementioned IG-HDR series. Our low toxicity rates, on the other hand, are comparable.

Despite its effectiveness and tolerability in a wide variety of anatomic locations, the optimal indication for IG-HDR remains unclear. Both EBRT and interventional radiology-ablation techniques have been well-studied and afford excellent probabilities of obtaining LC. However, many of the lesions in our series were either close to major vessels, close to other critical structures, and/or had a large diameter – all issues that can limit the appropriateness of either EBRT or interventional radiology-ablation techniques [3, 4, 5, 6, 7, 8]. In a recent dosimetric study comparing stereotactic body radiation therapy (SBRT) and IG-HDR plans for liver lesions, investigators found that IG-HDR could provide intra-tumoral dose escalation and decreased low dose spill to surrounding tissues [35]. On the other hand, for small lesions, SBRT may be preferred. For example, Rwigema *et al.* reported a one-year LC rate of 100% following the use of SBRT for 44 unresectable nodal and soft-tissue oligometatases [36]. The median gross tumor volume was 18.7 ml, considerably smaller than that in our study. Thus, IG-HDR may be most ideal in situations where other means of obtaining LC are relatively or absolutely contraindicated, as in the case of large lesion and/or lesions in close proximity to critical OARs.

Because of the small sample size, we did not attempt any statistical test to compare LC probabilities on the basis of anatomic site, EQD_2, or combination with EBRT vs. IG-HDR alone. It is probable that the relatively improved LC with combination EBRT relates to the fact that most patients treated with IG-HDR alone had relative contraindications to combination EBRT. Further study will be needed to determine the adequate dose and fractionation for IG-HDR cases.

There are several limitations to this work. First, the treated population is heterogeneous, rendering it difficult to make firm conclusions about the efficacy of IG-HDR. The primary goal of this work was to determine the efficacy and safety of escalated doses of radiation in challenging treatment situations. Second, the employed definition of LC was based upon RECIST classification of treated lesions. Several patients had significant burden of disease and IG-HDR was performed with a goal of symptomatic relief. While at least one follow-up imaging study was required for inclusion in this report, several patients did not obtain further imaging, nor did we feel it was appropriate to request them to do so solely for this study. Thus, it is possible that some patients had LC for a longer interval than was reported here. Conversely, it is possible that post-treatment hyperemia could have obscured the clear identification of a local failure; however, all images were reviewed by radiologists trained in utilizing the RECIST criteria. Additionally, our data appear to show a strong dose-response relationship with higher EQD_2 values associated with improved LC. As a result, one might argue that the patients who experienced poor LC in our study were underdosed. This may indeed be the case; as no clear OAR constraints and IG-HDR dosing guidelines were available for the relevant target locations at the time these patients were treated, doses were often chosen conservatively. Finally, the intention of IG-HDR as described herein is not to supplant other, more commonly used, and widely accessible ablative techniques but rather to provide an option in cases, for which those techniques may not be optimal.

Conclusions

In conclusion, IG-HDR appears to be an effective and safe joint interventional radiology/radiation oncology technique for achieving LC in patients with complex tumor masses, for which other ablative techniques are relatively contraindicated. Likely candidate lesions will be those that are large and/or in close proximity to critical structures or vessels.

Disclosure

Authors report no conflict of interest.

References

1. Corbin KS, Hellman S, Weichselbaum RR. Extracranial oligometastases: a subset of metastases curable with stereotactic radiotherapy. *J Clin Oncol* 2013; 31: 1384-1390.
2. Videtic GM. The role of stereotactic radiotherapy in the treatment of oligometastases. *Curr Oncol Rep* 2014; 16: 391.
3. Kim YS, Rhim H, Cho OK et al. Intrahepatic recurrence after percutaneous radiofrequency ablation of hepatocellular carcinoma: analysis of the pattern and risk factors. *Eur J Radiol* 2006; 59: 432-441.
4. Lam VW, Ng KK, Chok KS et al. Risk factors and prognostic factors of local recurrence after radiofrequency ablation of hepatocellular carcinoma. *J Am Coll Surg* 2008; 207: 20-29.
5. Tashiro H, Aikata H, Waki K et al. Treatment strategy for early hepatocellular carcinomas: comparison of radiofrequency ablation with or without transcatheter arterial chemoembolization and surgical resection. *J Surg Oncol* 2011; 104: 3-9.
6. Park HS, Harder EM, Mancini BR, Decker RH. Central versus Peripheral Tumor Location: Influence on Survival, Local Control, and Toxicity Following Stereotactic Body Radiotherapy for Primary Non-Small-Cell Lung Cancer. *J Thorac Oncol* 2015; 10: 832-837.
7. Osmundson EC, Wu Y, Luxton G et al. Predictors of toxicity associated with stereotactic body radiation therapy to the central hepatobiliary tract. *Int J Radiat Oncol Biol Phys* 2015; 91: 986-994.
8. Kim DW, Cho LC, Straka C et al. Predictors of rectal tolerance observed in a dose-escalated phase 1-2 trial of stereotactic body radiation therapy for prostate cancer. *Int J Radiat Oncol Biol Phys* 2014; 89: 509-517.
9. Lukens JN, Gamez M, Hu K, Harrison LB. Modern brachytherapy. *Semin Oncol* 2014; 41: 831-847.

10. Ricke J, Wust P, Stohlmann A et al. CT-guided interstitial brachytherapy of liver malignancies alone or in combination with thermal ablation: phase I-II results of a novel technique. *Int J Radiat Oncol Biol Phys* 2004; 58: 1496-1505.
11. Ricke J, Wust P, Wieners G et al. Liver malignancies: CT-guided interstitial brachytherapy in patients with unfavorable lesions for thermal ablation. *J Vasc Interv Radiol* 2004; 15: 1279-1286.
12. Rühl R, Lüdemann L, Czarnecka A et al. Radiobiological restrictions and tolerance doses of repeated single-fraction hdr-irradiation of intersecting small liver volumes for recurrent hepatic metastases. *Radiat Oncol* 2010; 5: 44.
13. Collettini F, Schnapauff D, Poellinger A et al. Hepatocellular carcinoma: computed-tomography-guided high-dose-rate brachytherapy (CT-HDRBT) ablation of large (5-7 cm) and very large (> 7 cm) tumours. *Eur Radiol* 2012; 22: 1101-1109.
14. Tselis N, Chatzikonstantinou G, Kolotas C et al. Hypofractionated accelerated computed tomography-guided interstitial high-dose-rate brachytherapy for liver malignancies. *Brachytherapy* 2012; 11: 507-514.
15. Collettini F, Singh A, Schnapauff D et al. Computed-tomography-guided high-dose-rate brachytherapy (CT-HDRBT) ablation of metastases adjacent to the liver hilum. *Eur J Radiol* 2013; 82: e509-514.
16. Tselis N, Chatzikonstantinou G, Kolotas C et al. Computed tomography-guided interstitial high dose rate brachytherapy for centrally located liver tumours: a single institution study. *Eur Radiol* 2013; 23: 2264-2270.
17. Brinkhaus G, Lock JF, Malinowski M et al. CT-guided high-dose-rate brachytherapy of liver tumours does not impair hepatic function and shows high overall safety and favourable survival rates. *Ann Surg Oncol* 2014; 21: 4284-4292.
18. Collettini F, Lutter A, Schnapauff D et al. Unresectable colorectal liver metastases: percutaneous ablation using CT-guided high-dose-rate brachytherapy (CT-HDBRT). *Rofo* 2014; 186: 606-612.
19. Denecke T, Stelter L, Schnapauff D et al. CT-guided Interstitial Brachytherapy of Hepatocellular Carcinoma before Liver Transplantation: an Equivalent Alternative to Transarterial Chemoembolization? *Eur Radiol* 2015; 25: 2608-2616.
20. Sharma DN, Thulkar S, Sharma S et al. High-dose-rate interstitial brachytherapy for liver metastases: first study from India. *J Contemp Brachytherapy* 2013; 5: 70-75.
21. Bishop AJ, Gupta S, Cunningham MG et al. Interstitial Brachytherapy for the Treatment of Locally Recurrent Anorectal Cancer. *Ann Surg Oncol* 2015 Apr 24 [Epub ahead of print].
22. Wang Z, Lu J, Liu L et al. Clinical application of CT-guided (125)I seed interstitial implantation for local recurrent rectal carcinoma. *Radiat Oncol* 2011; 6: 138.
23. Wang JJ, Yuan HS, Li JN et al. Interstitial permanent implantation of 125I seeds as salvage therapy for re-recurrent rectal carcinoma. *Int J Colorectal Dis* 2009; 24: 391-399.
24. Wang JJ, Yuan HS, Li JN et al. CT-guided radioactive seed implantation for recurrent rectal carcinoma after multiple therapy. *Med Oncol* 2010; 27: 421-429.
25. Tselis N, Ferentinos K, Kolotas C et al. Computed tomography-guided interstitial high-dose-rate brachytherapy in the local treatment of primary and secondary intrathoracic malignancies. *J Thorac Oncol* 2011; 6: 545-552.
26. Kolotas C, Tselis N, Sommerlad M et al. Reirradiation for recurrent neck metastases of head-and-neck tumors using CT-guided interstitial 192Ir HDR brachytherapy. *Strahlenther Onkol* 2007; 183: 69-75.
27. Rudžianskas V, Inčiūra A, Vaitkus S et al. Reirradiation for patients with recurrence head and neck squamous cell carcinoma: a single-institution comparative study. *Medicina (Kaunas)* 2014; 50: 92-99.
28. Jiang YL, Meng N, Wang JJ et al. Percutaneous computed tomography/ultrasonography-guided permanent iodine-125 implantation as salvage therapy for recurrent squamous cell cancers of head and neck. *Cancer Biol Ther* 2010; 9: 959-966.
29. Hepel JT, Syed AM, Puthawala A et al. Salvage high-dose-rate (HDR) brachytherapy for recurrent head-and-neck cancer. *Int J Radiat Oncol Biol Phys* 2005; 62: 1444-1450.
30. Bretschneider T, Mohnike K, Hass P et al. Efficacy and safety of image-guided interstitial single fraction high-dose-rate brachytherapy in the management of metastatic malignant melanoma. *J Contemp Brachytherapy* 2015; 7: 154-160.
31. Hall EJ, Giaccia AJ. Radiobiology for the radiologist. 7th ed. Lippincott Williams & Wilkins, Philadelphia 2011.
32. Institute NC. Common Terminology Criteria for Adverse Events (CTCAE) version 4 system 2010 [cited 2015 April 15]. Available from: http://evs.nci.nih.gov/ftp1/CTCAE/CTCAE_4.03_2010-06-14_QuickReference_5x7.pdf
33. Eisenhauer EA, Therasse P, Bogaerts J et al. New response evaluation criteria in solid tumours: revised RECIST guideline (version 1.1). *Eur J Cancer* 2009; 45: 228-247.
34. Pollom E, Deng L, Pai RK et al. Gastrointestinal toxicities with combined anti-angiogenic and stereotactic body radiation therapy. *Int J Radiat Oncol Biol Phys* 2015; 92: 568-576.
35. Pennington JD, Park SJ, Abgaryan N et al. Dosimetric comparison of brachyablation and stereotactic ablative body radiotherapy in the treatment of liver metastasis. *Brachytherapy* 2015; 14: 537-542.
36. Rwigema JC, King C, Wang PC et al. Stereotactic body radiation therapy for abdominal and pelvic oligometastases: Dosimetric targets for safe and effective local control. *Pract Radiat Oncol* 2015; 5: e183-191.